

Enhancing optical extreme events through input wave disorder

D. Pierangeli,^{1,*} G. Musarra,¹ F. Di Mei,¹ G. Di Domenico,¹ A. J. Agranat,² C. Conti,^{1,3} and E. DelRe¹

¹*Dipartimento di Fisica, Università di Roma “La Sapienza”, 00185 Rome, Italy*

²*Applied Physics Department, Hebrew University of Jerusalem, 91904 Jerusalem, Israel*

³*ISC-CNR, Università di Roma “La Sapienza”, 00185 Rome, Italy*

(Received 20 September 2016; published 15 December 2016)

We demonstrate how the emergence of extreme events strongly depends on the correlation length of the input field distribution. Observing the behavior of optical waves in turbulent photorefractive propagation with partially incoherent excitations, we find that rogue waves are strongly enhanced for a characteristic input correlation scale. Waveform analysis identifies this scale with a characteristic peak-intensity-independent wave size, suggesting a general role played by saturation in the nonlinear response in rogue phenomena.

DOI: [10.1103/PhysRevA.94.063833](https://doi.org/10.1103/PhysRevA.94.063833)

Great interest revolves around the study of anomalously large perturbations in wave systems since these profoundly affect their properties and response. Extreme amplitude events in hydrodynamic, acoustic, and optical wave dynamics, known as rogue waves, have been shown to present common features when different physical mechanisms specific for each system are involved in their generation [1]. Universal statistical traits and general model equations for rogue waves have fuelled particular research efforts in optics [2], where abnormal pulses can be exploited for applications [3] and various systems promise to be used as test benches to study the origin and properties of their not well understood oceanic counterparts [4,5]. Several physical ingredients underlying the occurrence of long-tail statistics have been identified, such as interacting coherent structures emerging from stochastic instabilities [6–11], interference for quasirandom wave fields [12–14], wave turbulence in incoherent nonlinear propagation [15–20], and spatiotemporal chaos in dissipative and cavity dynamics [21–26]. In highly nonlinear beam propagation, abnormal waves have been recently shown to emerge due to turbulent soliton dynamics [27,28]. However, fundamental issues such as the role of wave disorder and input field incoherence remain open.

Here we investigate the role of the spatial coherence scale on extreme events in spatially extended photorefractive propagation tailoring the spatial autocorrelation of a partially incoherent input field. In particular, we report a scale-dependent behavior of the long-tail statistics, which are greatly enhanced for a specific scale of the spatial incoherence. Remarkably, high-resolution measurements of the rogue waveforms reveal that these form with a characteristic intensity-independent size that coincides with the enhancing spatial incoherence scale. Using a photorefractive soliton-based model, this suggests a principal role played by saturation.

In our experiments we make use of partially incoherent beams propagating in photorefractive ferroelectrics, where rogue events have been observed through coherent one-dimensional input excitations [27]. Setup and methods are shown schematically in Fig. 1(a). They are based on the peculiar electro-optic features of disordered ferroelectric crystals in proximity of their structural phase transition [28–32]

and on the photorefractive propagation of partially incoherent beams [33,34]. Specifically, light at a wavelength $\lambda = 532$ nm from a 150-mW continuous-wave laser is expanded and focused on a glass diffuser plate, where transmitted radiation is collected producing a collimated speckle field. A long-working-distance objective (NA = 0.55) launches this field at the input facet of a photorefractive ferroelectric crystal of potassium-lithium-tantalate-niobate (KLTN), $\text{K}_{1-\alpha}\text{Li}_\alpha\text{Ta}_{1-\beta}\text{Nb}_\beta\text{O}_3$ ($\alpha = 0.04$, $\beta = 0.38$). The partially incoherent beam, linearly polarized in the experimental plane, copropagates with a background intensity along the z axis of the crystal and is detected at the output facet through a high-resolution imaging system (NA = 0.50) and a CCD camera. The sample is a zero-cut optical quality specimen with size $2.4^{(x)} \times 2.0^{(y)} \times 1.7^{(z)}$ mm³ ($l_x \times l_y \times l_z$) and with the ferroelectric transition occurring at the Curie temperature $T_C = 294$ K. Spatiotemporal fluctuations of the media response persist also slightly above this point so that disorder-affected light dynamics can be studied and controlled with high reproducibility at $T = T_C + 2$ K. Here, an external bias field is applied transversely to the propagation axis to tune the strength of the Kerr-saturated nonlinearity [35]. The incoherence properties of the input beam are achieved by placing the diffuser in between two confocal lenses (f_1 and f_2) and they are varied by changing its position along the propagation axis, whereas small tilts and rotations on it generate different disordered realizations of the optical field. Examples of partially incoherent beams at the crystal input and output are reported in Figs. 1(b) and 1(c) for two positions of the scatterer along the propagation axis. For the output intensity distribution we consider the spatial autocorrelation function

$$g(\Delta r) = \frac{\langle \int d^2r I(r)I(r + \Delta r) \rangle}{\int d^2r \langle I(r) \rangle \langle I(r + \Delta r) \rangle}, \quad (1)$$

whose width defines the spatial correlation length σ , i.e., the average speckle size. Since σ varies as nonlinear effects are involved in wave dynamics [36], we use the input source size S as a parameter characterizing the spatial incoherence of the input beam. We have $S \simeq 2\lambda l_z / g(0)\sigma$, which generalizes to nonlinear conditions optical speckle propagation [36,37].

In Fig. 2 the detected probability distribution function (PDF) of the output intensity is reported varying the beam

*davide.pierangeli@roma1.infn.it

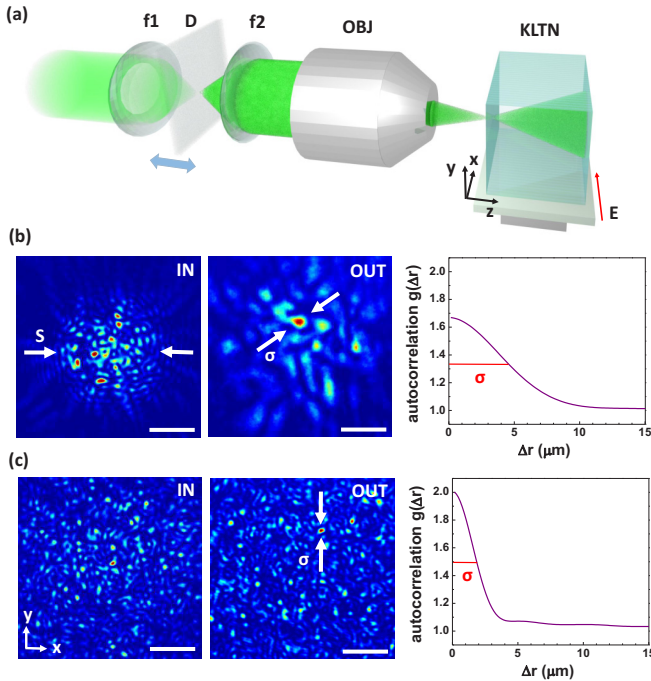


FIG. 1. Partially incoherent beams in photorefractive ferroelectric crystals. (a) Sketch of the experimental setup with lenses ($f_1 = f_2 = 50$ mm), adjustable glass diffuser D (average particle size of $2 \mu\text{m}$), long-working-distance objective OBJ (NA = 0.55) and KLTN sample. (b)–(c) Input and output intensities with the corresponding spatial autocorrelation function $g(\Delta r)$ for two different positions of the scatterer. σ indicates the output autocorrelation length and S is the corresponding input source size. Scale bars correspond to $30 \mu\text{m}$.

incoherence both in the linear and nonlinear case. In linear conditions, where no external field is applied, we observe [Fig. 2(a)] no significant deviations from the Gaussian statistics as expected for completely random interfering waves [38]. The exponential scaling $\text{PDF} = \exp(-I/\langle I \rangle)/\langle I \rangle$ is well verified in particular for beams presenting spatial coherence only on

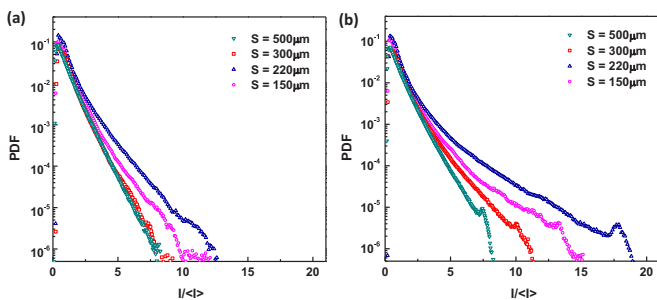


FIG. 2. Scale-dependent behavior of the intensity statistics. (a) PDF measured in linear conditions ($E = 0$, $P = 400 \mu\text{W}$) for beams with different coherent lengths expressed through the input parameter S . (b) Corresponding distributions for nonlinear propagation ($E = 2$ kV/cm, $P = 400 \mu\text{W}$), showing a long-tail behavior depending on the specific correlation length, with a large enhancement in rogue-wave appearance for $S = 220 \mu\text{m}$. Suppression of the tail occurs for highly incoherent fields ($S = 500 \mu\text{m}$).

small scales ($S \approx 500$, $S \approx 300 \mu\text{m}$). For more correlated beams ($S \approx 220$, $S \approx 150 \mu\text{m}$), the PDF slightly deviates at large intensities, consistently with the presence of weak inhomogeneities in the phases of the elementary interfering waves [12,14]. Rogue waves occur as the nonlinearity is activated by means of the external field $E = 2$ kV/cm. In the nonlinear case, the incoherent field experiences strong self-interaction and spatiotemporal fluctuations so we observe the speckle intensity dynamically varying in a turbulent fashion [28].

To study the statistics in this stage, we acquire more than 200 independent spatial distributions for a fixed $400 \mu\text{W}$ input power and sample conditions. Results as a function of the coherence length are shown in Fig. 2(b) and demonstrate how extreme events strongly depend upon this parameter. We found the long-tail statistics defining rogue waves and a peculiar scale-dependent behavior. Specifically, the spatial correlation scale of the optical field strongly affects its PDF, with a large enhancement in extreme event appearance that occurs for incoherent beams of size $S \approx 220 \mu\text{m}$ and their complete suppression at $S \approx 500 \mu\text{m}$. We note that the effect is approximately independent of the input power and of the value of the applied field, provided that both are above a certain threshold ensuring the highly nonlinear dynamics. Therefore, we observe that small-scale random intensity fluctuations inhibit rogue-wave generation, whereas a peculiar increase in their probability is triggered by a specific input disorder scale. We note that a similar inhibition for highly incoherent waves has been also reported in the temporal turbulent dynamics of a passive optical fiber ring cavity [19].

To investigate the mechanism underlying the correlation between abnormal wave statistics and incoherence scale, we use our ability to resolve the spatial waveform of each event with $0.3 \mu\text{m}$ resolution (for typical wave features of $10 \mu\text{m}$). We first consider the data set with incoherence corresponding to the maximum statistical-tail enhancement and, in particular, we analyze the rogue-wave peak intensity I_P and its full-width-at-half-maximum ΔX . Examples of spatially resolved rogue waveforms emerging from partially incoherent intensity distributions are shown in Fig. 3(b) as giant pulses. In Fig. 3(a) we report an interesting behavior that is found for the two analyzed parameters: even though the abnormal waves span different peak intensities, their widths are almost constant. Localized events appear with the same transverse size irrespective of the fact that they populate the Gaussian portion of the PDF or the extreme one of its abnormal tail. This feature persists also at different bias fields and, as further shown in the following, it amounts to a general property of rogue waves in the saturable nonlinearity.

Therefore, we extend our analysis taking into account the width of the extreme events as a function of the degree of incoherence of the corresponding optical field. Specifically, we compare their typical scale ΔX with the correlation scale σ of its entire intensity distribution, obtained in the nonlinear regime according to Eq. (1). This allows us to inspect whether the rogue wave has a size determined by the mean autocorrelation length of the speckle beam or an intrinsic property is involved. The whole picture is presented in Fig. 4. Extreme events are found to emerge on a typical scale that is significantly lower or higher than the coherence

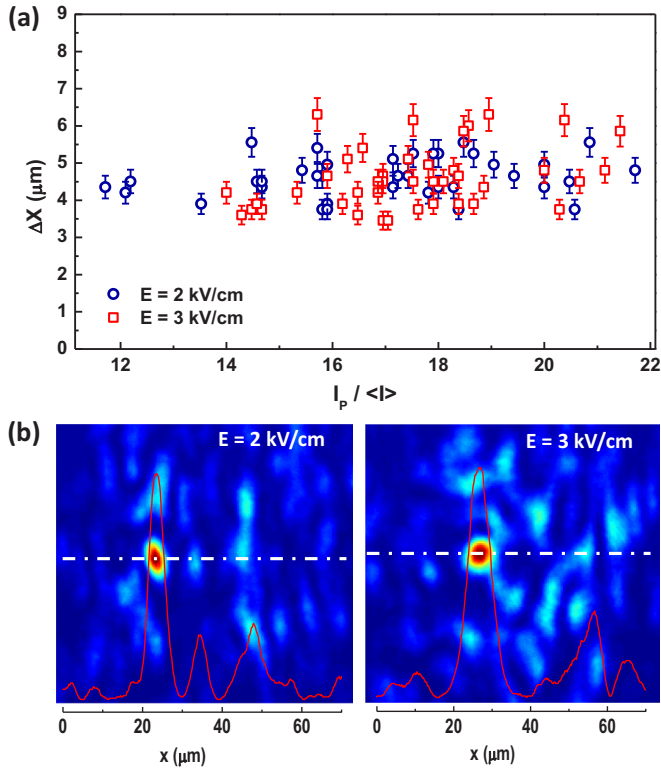


FIG. 3. Unveiling optical rogue waveforms. (a) Detected transverse width ΔX and peak intensity I_p of extreme events for data at different applied fields. (b) High-resolution spatial intensity distributions containing localized abnormal waveforms. Red curves are x -profiles along the dotted lines.

one, respectively, for beams of size $S = 150$ and $S = 300 \mu\text{m}$ [see Fig. 2(b)]. Moreover, matching between these two scales is evident at $S = 220 \mu\text{m}$, which is exactly the case in which the large enhancement in the long-tail statistics is detected. The findings prove that the key feature providing the optimal input disorder conditions for the emergence of non-Gaussian statistics is the existence of an intrinsic scale for rogue waves. We estimate it to be approximately $\overline{\Delta X} = 4.5 \mu\text{m}$. In fact, as schematically illustrated in Fig. 4, the coherence length distribution of the input beam acts as a probe for the probability $P(\Delta X)$ of finding extreme events with a certain width ΔX . Their overlap, in terms of size, sets the amount of emerging extreme events, so that the enhancement at $S = 220 \mu\text{m}$ appears as a resonant interaction.

The existence of a preferential size for extreme waves provides key information needed to understand statistically their appearance. Moreover, once the nonlinear propagation conditions are fixed, the spatial correlation of the optical field can be tuned to arbitrarily modify the intensity distribution tail. The generality of this mechanism relies on the physical basis that leads to a typical size for rogue events. We address the fundamental question on its origin starting from the consideration that the main properties of the photorefractive nonlinearity underlying our optical dynamics is its saturable character. Since saturation turns out in the response of any real system for large excitations, the finding may represent a universal trait in abnormal wave events, at least in this

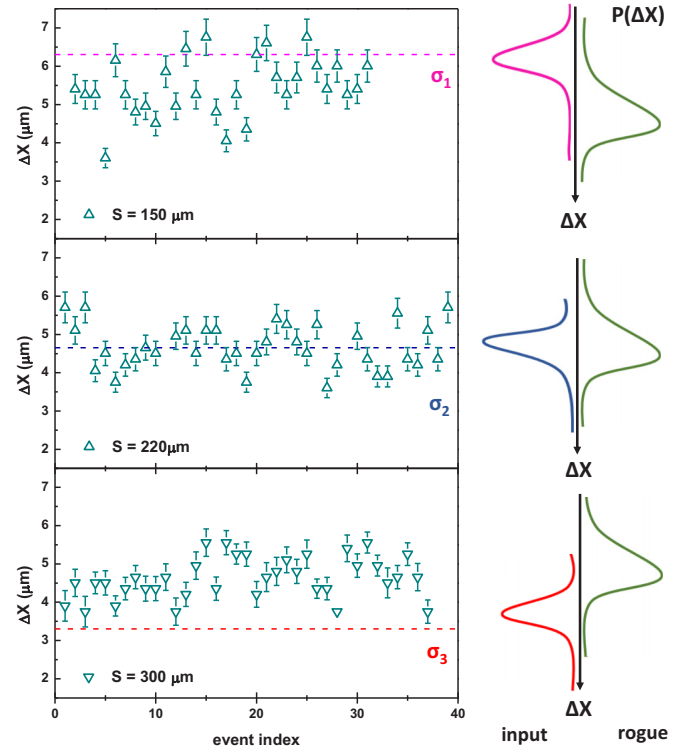


FIG. 4. Evidence of a typical scale in rogue waveforms. Measured extreme event widths at different coherence lengths σ (dashed lines). The two scales are resonant for $S = 220 \mu\text{m}$, where a large increase results in the probability of rogue-wave appearance [see main text and Fig. 2(b)]. The diagram on the right illustrates how results imply the presence of a typical spatial scale for rogue events.

limit condition. For our system, we here provide a physical picture that explains not only the presence of a peculiar spatial scale, but also the observed insensitivity to wave intensity. The framework is based on spatial solitons in saturable nonlinearities, whose structural and interaction properties have been suggested to play a key role in rogue waves in these media [27]. We consider their nonequilibrium counterpart, i.e., transient self-trapping waves in nonstationary conditions [39]. As detailed in Ref. [40], in the present case, transverse localization occurs on a size

$$\Delta x \simeq \frac{3\lambda}{2\pi n^2 a_{\text{eo}}} E^{-2}, \quad (2)$$

where n is the linear index of refraction and a_{eo} a parameter quantifying the electro-optical response of the media. For our experimental realization, we have $\Delta x = 5 \pm 1 \mu\text{m}$, where the uncertainty is related to the uncertainty in a_{eo} in proximity of the ferroelectric phase transition for biased condition [29]. This value of Δx is consistent with the typical scale of rogue waveforms $\overline{\Delta X}$ we have found. Moreover, Eq. (2) possesses the fundamental property of being independent of the wave intensity, in agreement with our observations of extreme events [Fig. 3(a)]. Dependence on the external electric field E is predicted as very weak at high values, and the result in Fig. 3(a) with different bias fields verifies this feature. Therefore, observations strongly suggest that the scale dependence of long-tail statistics with spatial incoherence can be explained

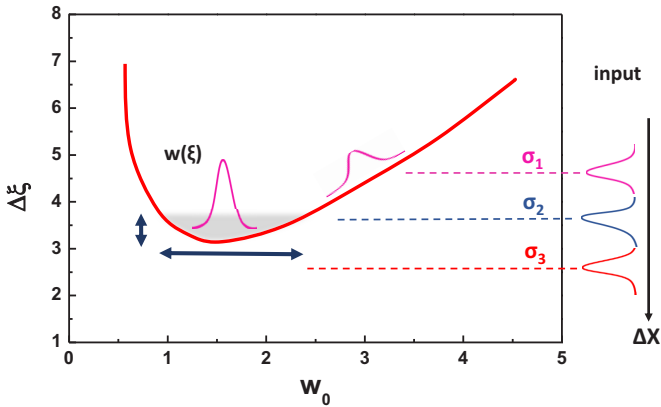


FIG. 5. Possible mechanism underlying the appearance of extreme intensity fluctuations. Existence curve of nonequilibrium solitons in saturable nonlinearities (red line) on which the waveform $w(\xi)$ is schematically shown. Arrows indicate the magnitude of width and amplitude fluctuations in the gray region, which is in proximity of the localized, self-trapped, wave solution. For comparison with Figs. 4 and 2, input correlation lengths used in experiments are also reported.

with the mechanism illustrated in Fig. 5, where the phase-space of the nonlinear waves in terms of normalized amplitude w_0 and width $\Delta\xi$ is recalled. Nonequilibrium self-trapped waves form across the minimum of the existence curve according

to Eq. (2) [40]. Here, a small variation in $\Delta\xi$ can lead to large fluctuations of the wave amplitude, with peak intensities reaching the giant values that populate the extreme regions of the total PDF. Extreme events are enhanced when the input coherence scale falls in this region, whereas their excitations and suppression implies, respectively, that matching with the input autocorrelation is partial or does not occur at all.

Summarizing, we have experimentally investigated the role of input wave disorder in the formation of optical extreme events. Exploiting highly nonlinear propagation of partially incoherent beams in photorefractive ferroelectric crystals, we reveal how the occurring of abnormal events strongly depends on the coherence length of the optical field. Tuning the input spatial autocorrelation we are able to modify the long-tail statistics of the output intensity distribution from inhibition to large enhancement. In our specific case, we are able to attribute this scale-dependent property to the onset of saturation in the nonlinearity.

Our results show how input disorder can be harnessed to enhance rogue phenomena and suggest that saturation may form a fundamental element in solving the extreme wave puzzle, thus requiring the high-resolution analysis of extreme event waveforms in other systems, from water waves to light pulses in fibers.

We acknowledge funding from grants PRIN 2012BFNWZ2 and the Sapienza 2014-2015 Awards Projects.

- [1] M. Onorato, S. Residori, U. Bortolozzo, A. Montina, and F. T. Arecchi, Rogue waves and their generating mechanisms in different physical contexts, *Phys. Rep.* **528**, 47 (2013).
- [2] D. R. Solli, C. Ropers, P. Koonath, and B. Jalali, Optical rogue waves, *Nature* **450**, 1054 (2007).
- [3] M. Leonetti and C. Conti, Observation of three dimensional optical rogue waves through obstacles, *Appl. Phys. Lett.* **106**, 254103 (2015).
- [4] T. A. Adcock and P. H. Taylor, The physics of anomalous ('rogue') ocean waves, *Rep. Prog. Phys.* **77**, 105901 (2014).
- [5] F. Fedele, J. Brennan, S. P. de Len, J. Dudley, and F. Dias, Real world ocean rogue waves explained without the modulational instability, *Sci. Rep.* **6**, 27715 (2016).
- [6] J. M. Dudley, F. Dias, M. Erkintalo, and G. Genty, Instabilities, breathers and rogue waves in optics, *Nat. Photon.* **8**, 755 (2014).
- [7] M. Onorato *et al.*, Statistical Properties of Directional Ocean Waves: The Role of the Modulational Instability in the Formation of Extreme Events, *Phys. Rev. Lett.* **102**, 114502 (2009).
- [8] M. Shats, H. Punzmann, and H. Xia, Capillary Rogue Waves, *Phys. Rev. Lett.* **104**, 104503 (2010).
- [9] S. Birkholz, E. T. J. Nibbering, C. Bree, S. Skupin, A. Demircan, G. Genty, and G. Steinmeyer, Spatiotemporal Rogue Events in Optical Multiple Filamentation, *Phys. Rev. Lett.* **111**, 243903 (2013).
- [10] C. Lecaplain, Ph. Grelu, J. M. Soto-Crespo, and N. Akhmediev, Dissipative Rogue Waves Generated by Chaotic Pulse Bunching in a Mode-Locked Laser, *Phys. Rev. Lett.* **108**, 233901 (2012).
- [11] A. Armaroli, C. Conti, and F. Biancalana, Rogue solitons in optical fibers: A dynamical process in a complex energy landscape? *Optica* **2**, 497 (2015).
- [12] F. T. Arecchi, U. Bortolozzo, A. Montina, and S. Residori, Granularity and Inhomogeneity Are the Joint Generators of Optical Rogue Waves, *Phys. Rev. Lett.* **106**, 153901 (2011).
- [13] R. Hohmann, U. Kuhl, H.-J. Stickmann, L. Kaplan, and E. J. Heller, Freak Waves in the Linear Regime: A Microwave Study, *Phys. Rev. Lett.* **104**, 093901 (2010).
- [14] C. Liu, R. E. C. van der Wel, N. Rotenberg, L. Kuipers, T. F. Krauss, A. Di Falco, and A. Fratalocchi, Triggering extreme events at the nanoscale in photonic seas, *Nat. Phys.* **11**, 358 (2015).
- [15] A. N. Ganshin, V. B. Efimov, G. V. Kolmakov, L. P. Mezhdogdin, and P. V. McClintock, Observation of an Inverse Energy Cascade in Developed Acoustic Turbulence in Superfluid Helium, *Phys. Rev. Lett.* **101**, 065303 (2008).
- [16] K. Hammani, B. Kibler, C. Finot, and A. Picozzi, Emergence of rogue waves from optical turbulence, *Phys. Lett. A* **374**, 3585 (2010).
- [17] P. Walczak, S. Randoux, and P. Suret, Optical Rogue Waves in Integrable Turbulence, *Phys. Rev. Lett.* **114**, 143903 (2015).
- [18] S. Randoux, P. Walczak, M. Onorato, and P. Suret, Nonlinear random optical waves: Integrable turbulence, rogue waves and intermittency, *Physica D (Amsterdam)* **333**, 323 (2016).
- [19] M. Conforti, A. Mussot, J. Fatome, A. Picozzi, S. Pitois, C. Finot, M. Haelterman, B. Kibler, C. Michel, and G. Millot, Turbulent dynamics of an incoherently pumped passive optical fiber cavity: Quasisolitons, dispersive waves, and extreme events, *Phys. Rev. A* **91**, 023823 (2015).

- [20] P. Suret, R. El Koussaifi, A. Tikan, C. Evain, S. Randoux, C. Szewaj, and S. Bielawski, Single-shot observation of optical rogue waves in integrable turbulence using time microscopy, *Nat. Commun.* **7**, 13136 (2016).
- [21] A. Montina, U. Bortolozzo, S. Residori, and F. T. Arecchi, Non-Gaussian Statistics and Extreme Waves in a Nonlinear Optical Cavity, *Phys. Rev. Lett.* **103**, 173901 (2009).
- [22] C. Bonatto, M. Feyereisen, S. Barland, M. Giudici, C. Masoller, J. R. Rios Leite, and J. R. Tredicce, Deterministic Optical Rogue Waves, *Phys. Rev. Lett.* **107**, 053901 (2011).
- [23] A. N. Pisarchik, R. Jaimes-Reategui, R. Sevilla-Escoboza, G. Huerta-Cuellar, and M. Taki, Rogue Waves in a Multistable System, *Phys. Rev. Lett.* **107**, 274101 (2011).
- [24] C. J. Gibson, A. M. Yao, and G. L. Oppo, Optical Rogue Waves in Vortex Turbulence, *Phys. Rev. Lett.* **116**, 043903 (2016).
- [25] N. Marsal, V. Caulet, D. Wolfersberger, and M. Sciamanna, Spatial rogue waves in a photorefractive pattern-forming system, *Opt. Lett.* **39**, 3690 (2014).
- [26] F. Selmi, S. Coulibaly, Z. Loghmari, I. Sagnes, G. Beaudoin, M. G. Clerc, and S. Barbay, Spatiotemporal Chaos Induces Extreme Events in an Extended Microcavity Laser, *Phys. Rev. Lett.* **116**, 013901 (2016).
- [27] D. Pierangeli, F. Di Mei, C. Conti, A. J. Agranat, and E. Del Re, Spatial Rogue Waves in Photorefractive Ferroelectrics, *Phys. Rev. Lett.* **115**, 093901 (2015).
- [28] D. Pierangeli, F. Di Mei, G. Di Domenico, A. J. Agranat, C. Conti, and E. DelRe, Turbulent Transitions in Optical Wave Propagation, *Phys. Rev. Lett.* **117**, 183902 (2016).
- [29] D. Pierangeli, F. Di Mei, J. Parravicini, G. B. Parravicini, A. J. Agranat, C. Conti, and E. DelRe, Observation of an intrinsic nonlinearity in the electro-optic response of freezing relaxors ferroelectrics, *Opt. Mat. Express* **4**, 1487 (2014).
- [30] D. Pierangeli, M. Ferraro, F. Di Mei, G. Di Domenico, C. E. M. de Oliveira, A. J. Agranat, and E. Del Re, Super-crystals in composite ferroelectrics, *Nat. Commun.* **7**, 10674 (2016).
- [31] E. DelRe, F. DiMei, J. Parravicini, G. B. Parravicini, A. J. Agranat, and C. Conti, Subwavelength anti-diffracting beams propagating over more than 1,000 Rayleigh lengths, *Nat. Photon.* **9**, 228 (2015).
- [32] F. DiMei, P. Caramazza, D. Pierangeli, G. Di Domenico, H. Ilan, A. J. Agranat, P. Di Porto, and E. Del Re, Intrinsic Negative Mass from Nonlinearity, *Phys. Rev. Lett.* **116**, 153902 (2016).
- [33] M. Mitchell, Z. Chen, M. F. Shih, and M. Segev, Self-Trapping of Partially Spatially Incoherent Light, *Phys. Rev. Lett.* **77**, 490 (1996).
- [34] Z. Chen, M. Segev, and D. N. Christodoulides, Experiments on partially coherent photorefractive solitons, *J. Opt. A: Pure Appl. Opt.* **5**, S389 (2003).
- [35] E. DelRe, B. Crosignani, and P. Di Porto, Photorefractive Solitons and Their Underlying Nonlocal Physics, *Prog. Opt.* **53**, 153 (2009).
- [36] Y. Bromberg, Y. Lahini, E. Small, and Y. Silberberg, Hanbury Brown and Twiss interferometry with interacting photons, *Nat. Photon.* **4**, 721 (2010).
- [37] S. Derevyanko and E. Small, Nonlinear propagation of an optical speckle field, *Phys. Rev. A* **85**, 053816 (2012).
- [38] J. W. Goodman, *Statistical Properties of Laser Speckle Patterns* (Springer, Berlin, 1975).
- [39] N. Fressengeas, D. Wolfersberger, J. Maufroy, and G. Kugel, Build up mechanisms of (1+1)-dimensional photorefractive bright spatial quasi-steady-state and screening solitons, *Opt. Commun.* **145**, 393 (1998).
- [40] E. DelRe and E. Palange, Optical nonlinearity and existence conditions for quasi-steady-state photorefractive solitons, *J. Opt. Soc. Am. B* **23**, 2323 (2006).